

RSC Advances



This is an *Accepted Manuscript*, which has been through the Royal Society of Chemistry peer review process and has been accepted for publication.

Accepted Manuscripts are published online shortly after acceptance, before technical editing, formatting and proof reading. Using this free service, authors can make their results available to the community, in citable form, before we publish the edited article. This *Accepted Manuscript* will be replaced by the edited, formatted and paginated article as soon as this is available.

You can find more information about *Accepted Manuscripts* in the [Information for Authors](#).

Please note that technical editing may introduce minor changes to the text and/or graphics, which may alter content. The journal's standard [Terms & Conditions](#) and the [Ethical guidelines](#) still apply. In no event shall the Royal Society of Chemistry be held responsible for any errors or omissions in this *Accepted Manuscript* or any consequences arising from the use of any information it contains.

Structural optimization of super-gelators derived from naturally-occurring mannose and their morphological diversity

Fumiyasu Ono,^{*a} Hisayuki Watanabe^{a,b} and Seiji Shinkai^c

^aAdvanced Materials Research Laboratory, Collaborative Research Division, Art, Science and Technology Center for Cooperative Research, Kyushu University, 4-1 Kyudai-Shinmachi, Nishi-ku, Fukuoka-city, Fukuoka 819-0388, Japan,

^bNissan Chemical Industries, Ltd., 10-1 Tsuboi-Nishi 2-chome, Funabashi-city, Chiba 274-8507, Japan

^cInstitute of Systems, Information Technologies and Nanotechnologies (ISIT), 4-1 Kyudai-Shinmachi, Nishi-ku, Fukuoka-city, Fukuoka 819-0388, Japan

The mannose derivatives, as low molecular-weight gelators, with various alkoxy substituents on the aromatic ring of methyl-4,6-*O*-benzylidene- α -D-mannopyranoside were synthesized. Most of these mannose derivatives could gel in various solvents such as octane, cyclohexane, toluene, ethylene glycol and ethanol solution at lower concentration than 2.0 wt%. In particular, *the critical gelation concentration (CGC) of methyl-4,6-O-(4-butoxybenzylidene)- α -D-mannopyranoside (2) for squalane was only 0.025 wt%, one of the lowest CGCs we have ever experienced.* The observations of xerogel by FE-SEM, TEM and AFM revealed that the length of alkoxy chain of the mannose derivatives influences the gel morphologies. Moreover, the toluene gels formed from the mannose derivatives **1-6** functionalized by a linear alkoxy group exhibited thixotropic properties. Interestingly, the gels of various solvents formed from methyl-4,6-*O*-(4-dodecyloxybenzylidene)- α -D-mannopyranoside (**6**) (with the longest alkoxy chain on the aromatic ring in this paper) indicated the thixotropic property. Thus, we confirmed that alkoxy groups on the aromatic ring exert noticeable effects on the gelation properties of these mannose derivatives.

Introduction

Gelators are materials capable of forming a gel structure, which can contain fluid in its three-dimensional network. Specifically, a hydrogel accommodates water whereas an oil gel or an organogel accommodates oil or organic solvent, respectively. Polymeric gels supported by the cross-linked three-dimensional network have been a primary class of studied gelator compounds. Recently, there has been a vibrant increase in studies on low molecular-weight gelators (LMWGs) that are constructed from self-assemblies of

low molecular-weight compounds. Because of the synthetic easiness and the diversity of self-assemblies, one can integrate various additional functions within the LMW supramolecular gels. These advantages are characteristics of LMWGs, not available with polymeric gels. The development of LMWGs has proceeded for both aqueous and organic solvents.^{1–12} One can expect that the continuing endeavour to develop LMWGs eventually results in their implementation into industrial, cosmetic, electronic, optical device, oil spill and medicinal applications.

A variety of physical properties inherent to LMWGs can be applied to integrate the unique functions within the gels. One of the most fundamental properties is the phase transition between the sol phase and the gel phase, which can be used as stimuli to control the imparted functions. It is possible to induce the phase transition by heat mode, mechanical mode, light mode, *etc.* In 1998, Shinkai group reported that sugars are useful as basic skeletons to design LMWGs, where the gels are stabilized owing to the hydrogen-bonding interaction among the OH groups.¹³ As sugars are naturally-occurring materials, one can expect to extend them to those purposes that require the environmentally-friendly properties and functions.^{14–19} For example, Jadhav *et al.* prepared gels using sorbitol or mannitol derivatives, which can selectively remove oil from an oil-water mixture,¹⁵ whereas Vidyasagar *et al.* reported that mannitol derivatives can form transparent self-standing oil gels applicable to the film processing.¹⁷

We previously reported the gelation ability of methyl-4,6-*O*-benzilidene- α -D-mannopyranoside (referred to as 'Bn' in this paper).^{13, 20–23} It was found that this mannose derivative can form gels accommodating various solvents: in particular, the property to gelate both water and certain organic solvents is very unique.^{13, 20–36} However, these gels formed from this mannose skeleton could be either clear or slightly opaque (*e.g.*, the toluene-loaded gel was slightly opaque; Figure 1, left). We newly synthesized a mannose derivative functionalized with a methoxy group at the *para* position of the aromatic ring and evaluated its gelation ability for toluene. Interestingly, this derivative resulted in a transparent toluene-loaded gel showing a thixotropic behaviour (Figure 1, right). The finding implies that the slight modification of the gelator structure largely changes the gelation ability.

Stimulated by this finding, we extensively studied the possible correlation lying between the structure of mannose derivatives as LMWGs and their physical gelation properties, such as critical gelation concentration, gel-sol phase transition temperature, thixotropic property, *etc.* Specifically, we investigated the influence of the structure of the alkoxy groups, such as linear versus branch, saturated versus unsaturated,

para-substituted versus *meta*-substituted on the aromatic ring, *etc.* (Figure 2).

Results and discussion

Synthesis of mannose-based gelators

The mannose derivatives for LMWGs were synthesized from the corresponding aromatic aldehydes in two steps (Figure 3). Several *O*-substituted aromatic aldehydes were synthesized from 4-hydroxybenzaldehyde and corresponding alkylbromides using K_2CO_3 as a base in DMF at 80 °C or 150 °C. The acetals (mannose derivative precursors) were synthesized by the reaction of corresponding aldehydes and trimethyl orthoformate in the presence of $Cu(BF_4)_2$ catalyst in methanol at room temperature (RT). The final acetal compounds were derived by the reaction of aldehydes and methyl- α -D-mannopyranoside, the reaction being catalysed by *p*-TsOH in DMF at RT under reduced pressure. The yields in this reaction were up to 55%. These products were characterized by 1H NMR, ^{13}C NMR and HRMS.

Gelation abilities

The gelation ability of mannose-based derivatives was determined for a range of 19 different solvents and 6 aqueous mixtures; in each case, 2.0–20 mg of mannose derivatives was submerged in 1.0–8.0 mL of the desired solvent in a sealed vial while being heated (Table 1). The sample vial was cooled to RT, then the sample vial was inverted after 1 h. We classified the obtained results as follows: a transparent gel, a translucent gel, an opaque gel, a precipitate and a clear solution or a suspension. The results are summarized in Table 1.

The abbreviations used for each mannose derivative are as follows: linear alkoxy groups, **1–6**; linear alkoxy group with terminal olefin, **7**; branched alkoxy group at the *para* position on the aromatic ring, **8**; cyclic alkoxy *para*-substituted on the aromatic ring, **9**; and methoxy group at the *meta* and *para* positions on the aromatic ring, **10**. Derivatives **1–8** served as gelators for linear and cyclic alkanes (octane, cyclohexane, squalane and squalene), aromatic solvent (toluene) and decamethylcyclopentasiloxane (DOW CORNING TORAY SH 245 FLUID, referred to as 'SH245' in this paper.). Surprisingly, the critical gelation concentration (CGC) of **2** for squalane was 0.025 wt%, one of the lowest CGCs we have ever experienced. In other words, this gel consists of 99.975 wt% squalane. In addition, **1–6** and **7** were able to gelate olive oil, isopropyl myristate (IPM) and even ethylene glycol (in spite of the protic solvent). Both **2** and **7** gelled water. On the other hand, **9** and **10** exhibited no gelation ability for any of these solvents.

As demonstrated in Figure 4, an inverse correlation of CGC and solvent polarity was demonstrated with six analogous gelators. We estimated the CGCs of **2** and **6** to be 0.5 wt% (14.1 mM) and 2.0 wt% (42.9 mM) in toluene, respectively. In contrast, The CGCs of **2** and **6** were estimated to be 2.0 wt% (56.4 mM) and 0.25 wt% (5.4 mM), respectively, in ethylene glycol. These apparently anomalous tendencies are rationalized in terms of the inversion of the aggregation modes between nonpolar solvents and polar solvents: that is, in toluene, the sugar moiety should occupy the core and the alkoxy group should cover the shell surface, whereas the core shell relation should be inverted. The gelation ability of mannose derivatives in DMSO/H₂O and EtOH/H₂O mixtures was also investigated using derivatives **1–6** and **7**. As demonstrated in Figure 5, the higher water-content mixtures are gelled more easily with shortening the length of the linear alkoxy chains.

Gel-sol phase transitions

In Figure 6, the gel-sol phase transition temperatures (T_{gel}) of **Bn**, **1–6** and **7** in toluene are plotted against the gelator concentration in order to compare their concentration-dependent gelation properties. When compared at the same concentration, the T_{gel} values always maintained the following order from the highest to the lowest: **7**, **1**, **2**, **Bn**, **3**, **4**, **5**, **6**. The T_{gel} values of **7**, **1** and **2** were higher than that of **Bn** unfunctionalized alkoxy groups on the aromatic ring. Additionally, since the T_{gel} of **7** was consistently higher than other mannose derivatives, the thermal stabilization of toluene gel is likely due to the π - π interaction occasionally observed between terminal olefins.³⁷

Morphology of xerogels

We investigated the morphologies of several organogels prepared from **2** and **6** with toluene, cyclohexane and a 50/50 (vol/vol) mixture of ethanol and a few hydrogels, using field emission scanning electron microscopy (FE-SEM), transmittance electron microscopy (TEM) and atomic force microscopy (AFM) (Figure 7). For the FE-SEM measurements, the xerogels were obtained by freezing and pumping the gel for 5–14 h. For the TEM measurements, the samples were obtained by dipping a carbon-coated copper grid into the gel and negatively staining it with 1% phosphotungstic acid (adjusted to pH 7). For the AFM measurements, a droplet of a toluene solution containing **2** or **6** at 0.02 wt% below the CGC value was placed on the highly-ordered pyrolytic graphite (HOPG). After 1 h, the substrates were dried in vacuum for more than 12 h.

The FE-SEM image of the xerogel prepared from **2** and cyclohexane displayed a three-dimensional entangled fibrous network of 10-20 nm in width, whereas that of **6** displayed a sheet-like structure. The FE-SEM images of the xerogels formed from both **2** and **6** with toluene displayed a sheet-like structure. For the TEM images of gels prepared with toluene, **2** displayed a fibrous network of 140-200 nm in width, whereas **6** displayed a flowing stream-like structure. Interestingly, the AFM image of dried sample for a toluene solution of **2** at 0.02 wt% below the CGC value also depicted the fibrous networks when observed with TEM. Similarly, the AFM image of **6** in toluene showed the flowing stream-like structure. These phenomena reveal that the rate of self-assembled processes consisted from mannose derivatives **2** and **6** is faster than the evaporation rate of toluene. In the previous work, the SEM image of the xerogel formed from **Bn** with toluene displayed the fibrous network.¹⁹ Whereas, those of **2** and **6** displayed the sheet-like structures because of bundled fibers created by the van der Waals interaction between alkoxy chains. Furthermore, the difference in the TEM images obtained from **2** and **6** attributable to the difference is the strength of the van der Waals interaction induced by length of alkoxy chains: that is, the TEM and FE-SEM images of the xerogels prepared from the cyclohexane gel and the toluene gel of **6** showed sheet-like and stream-like structures because of the more strong van der Waals interaction of **6** arising from the longer alkoxy chain than that of **2**. For the xerogels prepared with the ethanol/water mixture, the FE-SEM image of **2** displayed both short and long, thick fibrous networks of 130-180 nm in width, whereas that of **6** displayed right-handed helical fibrous structures of 200-400 nm in width. These images were also observed for their corresponding TEM images. The FE-SEM and TEM images of the xerogel prepared from the hydrogel of **2** displayed both short and long, bundled thick fibrous networks of 150-550 nm in width. These characteristic xerogel morphologies prepared from the hydrogel of **2** are created by the periodic structure corresponding to the hexagonal organization, which is evidenced by XRD measurements described in the next chapter.

XRD measurements

The X-ray diffraction (XRD) pattern of the xerogels prepared from **2** and water showed periodical reflection peaks (Figure 8), which indicate that **2** indeed assembles into a hexagonal organization. The obtained long spacing distances (d) were 2.27 nm, 1.31 nm, 1.14 nm, 0.85 nm, 0.75 nm and 0.65 nm, which correspond to the ratios of 1:1, $\sqrt{3}$:1, 2:1, $\sqrt{7}$:1, 3:1 and $\sqrt{12}$:1, respectively. The 2.27 nm length is shorter than twice that of the extended molecular length of **2** (1.78 nm by CPK molecular modelling) but longer

than the length of one molecule. The aqueous gels prepared from **2**, therefore, should maintain an interdigitated bilayer structure with a thickness of 2.27 nm (Figure 9). This value is compatible with a bilayer structure that has the alkoxy chain tilted with respect to a normal vector of the layer's plane. In addition, the wide-angle region of the X-ray diagram for the hydrogel of **2** revealed a series of sharp reflection peaks. This finding supports the view that the long alkoxy chain groups form the highly ordered interdigitated layer packing stabilized by the hydrophobic interaction.

In contrast, the XRD diagram of the xerogel of **2** and toluene is remarkably different from that obtained in water; it has two broad peaks appearing at $d = 4.26$ and 2.03 nm in the small-angle region and one broad reflection peak in the wide-angle region. The main peak at 2.03 nm suggests an ordered arrangement of gelators in the fibrous structure. The weak peaks appearing at 4.26 and 0.62 nm are attributed to the bundled main fibers and the mannose moiety (self-organized by hydrogen bonding), respectively.

Next, we used XRD to measure the long spacing distances of **2**, **4** and **6** in xerogels prepared from toluene (Figure 10). The peaks appeared at 2.27 nm, 2.35 nm and 2.96 nm, respectively, indicating that the fiber diameter becomes thicker with a increase in the length of the alkoxy chain attached to the aromatic ring.

Thixotropic behaviours

The thixotropic property is a phenomenon characteristically observed for LMWGs and has garnered considerable interest of gel scientists because of the significant relations with the some biological self-healing process such as muscular fibers and injured neural fibers and with industrial applications for the materials such as cosmetics, paints, biomaterials and foodstuffs.^{38–47} We examined this behaviour for derivatives **Bn**, **1–6** and **7** at the CGC (Figures 11 and 12). The toluene gels were permitted to rest for 1 h at RT after heating the mixture of mannose derivatives and then the shear stress was introduced via vortex mixing. After 1 h at RT, the sample vial was inverted. The samples prepared from **1–6** and **7** showed the regeneration of the gels, indicating that they possess thixotropic properties, whereas the sample prepared from **Bn** does not.

Furthermore, the thixotropic properties of several gels prepared from mannose derivatives **2** and **6** were examined in more detail (Figure 13). For **2**, the gels of toluene, olive oil, IPM and ethylene glycol indicated thixotropic properties, whereas those of octane, cyclohexane and SH245 did not. Interestingly, the gels prepared from **6** exhibited the thixotropic property with octane, cyclohexane, toluene, SH245, olive oil,

IPM and ethylene glycol. Thixotropic processes undergo the self-assembled process from small pieces of fibers to the bundled fibers.⁴⁴ These results reveal that the self-assembled process was induced by the van der Waals interaction between alkoxy chains on the gelators. Especially, the van der Waals interaction of **6** (with the longest alkoxy chain among the mannose derivatives in this paper) between alkoxy chains on the gelators is the stronger than that of **2**. Therefore, **6** induced the thixotropic property of gels formed from various solvents compared to **2**.

Conclusions

We demonstrated that mannose derivatives with various alkoxy substituents are able to gelate organic solvents and protic solvents. Through this study, we have established that as a general tendency, the mannose derivatives bearing a short linear alkoxy chain tend to gelate the nonpolar solvents such as toluene and cyclohexane at the low concentration. On the other hand, those bearing a long linear alkoxy chain tend to gelate polar and protic solvents (*e.g.*, ethylene glycol) at the low concentration. Furthermore, LMWGs **2** and **6** exhibited thixotropic properties with a wide range of solvent groups. It thus has become clear that the proper alkoxy chain at the *para* position of the aromatic ring imparts transparency, stability and thixotropic behavior for the gels. We are now extending our research toward the functional application of these gels possessing unique physical properties. In future, we will report on the results obtained from these gels.

Experimental section

Apparatus for spectroscopic measurements

¹H and ¹³C NMR spectra were acquired on a JEOL JNM-ECA 600. Chemical shifts were reported in ppm from tetramethylsilane for ¹H NMR spectra and CDCl₃ for ¹³C NMR spectra as an internal standard. EI and FAB mass spectra were measured on a JEOL JMS-700.

Synthesis of Methyl-4,6-*O*-(4-butoxybenzylidene)- α -D-mannopyranoside (**2**)

Copper(II) tetrafluoroborate (48 mg, 0.2 mmol) was added to a mixture of 4-butoxybenzaldehyde (3.6 g, 20 mmol) and trimethyl orthoformate (4.4 mL, 40 mmol) in anhydrous methanol (8 mL) under nitrogen atmosphere. The reaction mixture was stirred for 1 h at RT. After 1 h, the reaction mixture was quenched with saturated NaHCO₃ and extracted with ethyl acetate. The extracts were washed with brine, dried over Na₂SO₄, filtered and concentrated under reduced pressure. The obtained clear oil

was afforded to the next reaction without further purification.

A solution of crude dimethylacetal in DMF (10 mL) was added dropwise to a suspension of methyl- α -D-mannopyranoside (4.3 g, 22 mmol) and p-toluenesulfonic acid (98 mg, 0.5 mmol) in anhydrous DMF (20 mL) under nitrogen atmosphere. The reaction mixture was stirred for 10 min at RT and for 2 h under reduced pressure at RT. After 2 h, the reaction mixture was quenched with saturated NaHCO₃ and extracted with ethyl acetate. The extracts were washed with brine, dried over Na₂SO₄, filtered and concentrated under reduced pressure. The crude product was purified by column chromatography (SiO₂; hexane/ethyl acetate from 70/30 to 50/50, vol/vol). The desired product, **2**, was obtained as a white solid (3.2 g, 45%).

Methyl-4,6-O-(4-butoxybenzylidene)- α -D-mannopyranoside (2). δ_{H} (600 MHz, CDCl₃): 7.40 (2H, d, $J = 8.5$ Hz), 6.89 (2H, d, $J = 8.8$ Hz), 5.52 (1H, s), 4.77 (1H, s), 4.31–4.22 (1H, m), 4.10–4.02 (2H, m), 3.96 (2H, t, $J = 6.6$ Hz), 3.93–3.86 (1H, m), 3.85–3.76 (2H, m), 3.40 (3H, s), 2.66–2.60 (2H, br), 1.80–1.71 (2H, m), 1.53–1.43 (2H, m), 0.97 (3H, t, $J = 7.6$ Hz). δ_{C} (150 MHz, CDCl₃): 159.86, 129.46, 127.51, 114.32, 102.29, 101.21, 78.81, 70.82, 68.82, 68.73, 67.75, 62.89, 55.10, 31.23, 19.20, 13.82. HRMS (EI⁺): m/z calc'd for C₁₈H₂₆O₇ (M⁺): 354.1679; found: 354.1682

The other mannose derivatives are described in the supporting information.

Gelation tests of organic solvents, mixed solvents and water

The gelator and the solvent were put in a sealed-capped vial and heated in an dry bath until the solid was dissolved. The solution was cooled at room temperature. If the stable gel was observed at this stage, it was classified as CGC values (wt%) in Table1.

Gel-sol phase transition temperatures

A sealed vial containing the gel was immersed in a thermostatic dry bath. In 5 °C increments, the sample vial was inverted and T_{gel} was defined as the temperature at which gel-sol consistency was observed.

TEM observations

TEM imaging was performed on a JEOL JEM-2010HCKM. The gel was prepared in a sample tube. For the TEM measurements, the samples were obtained by dipping a carbon-coated copper grid in the gel and dried in vacuum for more than 12 h. The dried grid was negative stained with 1% phosphotungstic acid adjusted to pH 7 for 5 or 10 min. The grids were washed with water and dried in vacuum for more than 12 h. The accelerating voltage of TEM was 200 kV.

SEM observations

FE-SEM imaging was performed on a Hitachi SU-8000 at the Center of Advanced Instrumental Analysis, Kyushu University. The xerogel of **1** was obtained by freezing and pumping a gel of **1** for 5–14 h. The obtained xerogel was thus not coated by metal. The accelerating voltage of SEM was less than 0.5 kV.

AFM observations

AFM was performed on an SII NanoTechnology Inc. Nanonavi/Nanocute (now Hitachi High-Tech Science Corp.). For the AFM measurements, a droplet of the solution of **2** or **6** at 0.02 wt% in toluene was placed on highly ordered pyrolytic graphite (HOPG). After 1 h, the substrates were dried in vacuum for more than 12 h.

XRD measurements

Powder XRD patterns were measured on a Rigaku RINT-TTR III X-ray diffractometer equipped with CuK α radiation (50 kV, 300 mA) at a scanning rate of 1°/min.

Acknowledgements

We thank Dr. Yumi Fukunaga for the support and valuable advice regarding TEM observations and Mr. Taisuke Matsumoto for the support of XRD measurements.

We thank Dr. Osamu Hirata and Dr. Akihiro Tanaka for their valuable comments and discussions.

References

- 1 P. Terech and R. G. Weiss, *Chem. Rev.*, 1997, **97**, 3133–3160.
- 2 O. Gronwald, E. Snip and S. Shinkai, *Curr. Opinion Colloid Int. Sci.*, 2002, **7**, 148–156.
- 3 L. A. Estroff and A. D. Hamilton, *Chem. Rev.*, 2004, **104**, 1201–1218.
- 4 N. M. Sangeetha and U. Maitra, *Chem. Soc. Rev.*, 2005, **34**, 821–836.
- 5 A. Ajayaghosh, V. K. Praveen and C. Vijayakumar, *Chem. Soc. Rev.*, 2008, **37**, 109–122.
- 6 A. R. Hirst, B. Escuder, J. F. Miravet and D. K. Smith, *Angew. Chem. Int. Ed.*, 2008, **47**, 8002–8018.
- 7 D. K. Smith, *Chem. Soc. Rev.*, 2009, **38**, 684–694.
- 8 M-O. M. Piepenbrock, G. O. Lloyd, N. Clarke and J. W. Steed, *Chem. Rev.*, 2010, **110**, 1960–2004.

- 9 A. Dawn, T. Shiraki, S. Haraguchi, S. Tamaru and S. Shinkai, *Chem. Asian. J.*, 2011, **6**, 266–282.
- 10 L. E. Buerkle and S. J. Rowan, *Chem. Soc. Rev.*, 2012, **41**, 6089–6102.
- 11 J. Raeburn, A. Z. Cardoso and D. J. Adams, *Chem. Soc. Rev.*, 2013, **42**, 5143–5156.
- 12 G. Yu, X. Yan, C. Han and F. Huang, *Chem. Soc. Rev.*, 2013, **42**, 6697–6722.
- 13 K. Yoza, Y. Ono, K. Yoshihara, T. Akao, H. Shinmori, M. Takeuchi, S. Shinkai and D. N. Reinhoudt, *Chem. Commun.*, 1998, **8**, 907–908.
- 14 J. Cui, A. Liu, Y. Guan, J. Zheng, Z. Shen and X. H. Wan, *Langmuir* 2010, **26**, 3615–3622.
- 15 S. R. Jadhav, P. K. Vemula, R. Kumar, S. R. Raghavan and G. John, *Angew. Chem. Int. Ed.*, 2010, **49**, 7695–7698.
- 16 G. Wang, H. Yang, S. Cheuk and S. Coleman, *Beilstein J. Org. Chem.*, 2011, **7**, 234–242.
- 17 A. Vidyasagar, K. Handore and K. M. Sureshan, *Angew. Chem. Int. Ed.* 2011, **50**, 8021–8024.
- 18 M. F. Abreu, V. T. Salvador, L. Vitorazi, C. E.N. Gatts, D. R. dos Santos, R. Giacomini, S. L. Cardoso and P. C.M.L. Miranda, *Carbohydr. Res.* 2012, **353**, 69–78.
- 19 E. Bedini, L. Cirillo and M. Parrilli, *Tetrahedron*, 2013, **69**, 1285–1296.
- 20 K. Yoza, N. Amanokura, Y. Ono, T. Akao, H. Shinmori, M. Takeuchi, S. Shinkai and D. N. Reinhoudt, *Chem. Eur. J.*, 1999, **5**, 2722–2729.
- 21 O. Gronwald, K. Sakurai, R. Luboradzki, T. Kimura and S. Shinkai, *Carbohydr. Res.* 2001, **331**, 307–318.
- 22 O. Gronwald and S. Shinkai, *J. Chem. Soc. Perkin Trans. 2*, 2001, 1933–1937.
- 23 O. Gronwald and S. Shinkai, *Chem. Eur. J.*, 2001, **7**, 4328–4334.
- 24 M. Mukai, H. Minamikawa, M. Aoyagi, T. Shimizu and M. Hogiso, *J. Colloid Interface Sci.*, 2000, **224**, 154–160.
- 25 J. H. Jung, G. John, M. Masuda, K. Yoshida, S. Shinkai and T. Shimizu, *Langmuir*, 2001, **17**, 7229–7232.
- 26 J. H. Jung, S. Shinkai and T. Shimizu, *Chem. Eur. J.* 2002, **8**, 2684–2690.
- 27 S. Kiyonaka, S. Shinkai and I. Hamachi, *Chem. Eur. J.* 2003, **9**, 976–983.
- 28 M. Suzuki, M. Yumoto, M. Kimura, H. Shirai and K. Hanabusa, *Helv. Chim. Acta* 2004, **87**, 1–10.
- 29 M. Suzuki, S. Owa, M. Kimura, A. Kurose, H. Shirai and K. Hanabusa, *Tetrahedron Lett.* 2005, **46**, 303–306.
- 30 M. Suzuki, M. Nanbu, M. Yumoto, H. Shirai and K. Hanabusa, *New J. Chem.* 2005, **29**, 1439–1444.

- 31 M. Suzuki, T. Sato, H. Shirai and K. Hanabusa, *New J. Chem.* 2007, **31**, 69–74.
- 32 S. Kiyonaka, S. Shinkai and I. Hamachi, *Chem. Eur. J.* 2003, **9**, 976–983.
- 33 Y. Imura, K. Matsue, H. Sugimoto, R. Ito, T. Kondo and T. Kawai, *Chem. Lett.* 2009, **38**, 778–779.
- 34 T. Kar, S. Debnath, D. Das, A. Shome and P. K. Das, *Langmuir*, 2009, **25**, 8639–8648.
- 35 N. Yan, G. He, H. Zhang, L. Ding and Y. Fang, *Langmuir*, 2010, **26**, 5909–5917.
- 36 N. Minakuchi, K. Hoe, D. Yamaki, S. Ten-no, K. Nakashima, M. Goto, M. Mizuhata and T. Maruyama, *Langmuir*, 2012, **28**, 9259–9266.
- 37 R. Wakabayashi, T. Ikeda, Y. Kubo, S. Shinkai and M. Takeuchi, *Angew. Chem. Int. Ed.*, 2009, **48**, 6667–6670.
- 38 D. M. Blow and A. Rich, *J. Am. Chem. Soc.*, 1960, **82**, 3566–3571.
- 39 J. Brinksma, B. L. Feringa, R. M. Kellog, R. Vreeker and J. van Esch, *Langmuir*, 2000, **16**, 9249–9255.
- 40 M. Lescanne, P. Grondin, A. d'Aleo, F. Fages, J.-L. Pozzo, O. M. Monval, P. Reinheimer and A. Colin, *Langmuir*, 2004, **20**, 3032–3041.
- 41 M. Shirakawa, N. Fujita and S. Shinkai, *J. Am. Chem. Soc.*, 2005, **127**, 4164–4165.
- 42 T. Shirosaki, S. Chowdhury, M. Takafuji, D. Alekperov, G. Popova, H. Hachisako and H. Ihara, *J. Mater. Res.* 2006, **21**, 1274–1278.
- 43 X. Huang, S. R. Raghavan, P. Terech and R. G. Weiss, *J. Am. Chem. Soc.*, 2006, **128**, 15341–15352.
- 44 P. Mukhopadhyay, N. Fujita, A. Takada, T. Kishida, M. Shirakawa and S. Shinkai, *Angew. Chem. Int. Ed.*, 2010, **49**, 6338–6342.
- 45 A. Shundo, K. Mizuguchi, M. Miyamoto, M. Goto and K. Tanaka, *Chem. Commun.*, 2011, **47**, 8844–8846.
- 46 X. Hou, D. Gao, J. Yan, Y. Ma, K. Liu and Y. Fang, *Langmuir*, 2011, **27**, 12156–12163.
- 47 H. Hoshizawa, Y. Minemura, K. Yoshikawa, M. Suzuki and K. Hanabusa, *Langmuir*, 2013, **29**, 14666–14673.



Figure 1. Images of toluene-filled gel formed from methyl-4,6-*O*-benzylidene- α -D-mannopyranoside (**Bn**) in a previous work (left) and **1** (right)

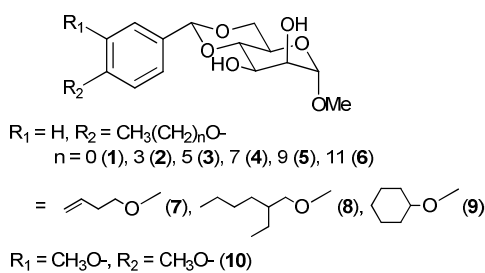


Figure 2. Structures of the investigated mannose derivatives in this study

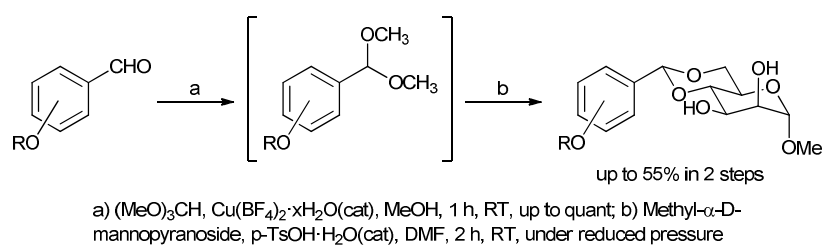


Figure 3. Synthetic scheme of mannose-based gelators

Table 1. The observed critical gelation concentration (CGC) values (wt%) and *qualitative note (qual. only if CGC could not be determined and CGC values only if the gel was transparent).

Entry	solvent	1	2	3	4	5	6	7	8	9	10
1	Octane	0.1	0.05	0.1	0.1	0.1	0.25	0.1 PG	0.05	IS	IS
2	Cyclohexane	0.25	0.05	0.05	0.1	0.1	0.1	0.1	0.25	IS	IS
3	Squalane	0.05	0.025 ***	0.05	0.05	0.05	0.1	0.05	0.1	IS	IS
4	Squalene	0.1	0.05	0.1	0.25	0.25	0.25	0.1	0.25	P	P
5	Toluene	0.5	0.5	1.0	1.0	2.0	2.0	0.5	S	IS	IS
6	SH245	0.05	0.05	0.05	0.1	0.25	0.5	0.05	0.1	IS	IS
7	Olive Oil	0.5	0.5	1.0	1.0	1.0	1.0	0.5	S	IS	P
8	IPM	0.5	0.5	1.0	1.0	1.0	1.0	0.5	S	IS	IS
9	Chloroform	S	S	S	S	S	S	S	S	S	S
10	Ethyl Acetate	S	S	S	S	S	S	S	S	S	S
11	Acetone	S	S	S	S	S	S	S	S	S	S
12	Cyclohexanone	S	S	S	S	S	S	S	S	S	S
13	Acetonitrile	S	S	S	S	S	S	S	S	P	S
14	DMSO	S	S	S	S	S	S	S	S	S	S
15	EtOH	S	S	S	S	S	S	S	S	S	S
16	MeOH	S	S	S	S	S	S	S	S	S	S
17	Ethylene Glycol	S	2.0 OG	2.0 TL	1.0 TL	0.5 TL	0.25 TL	S	P	S	S
18	Glycerol	S	2.0 TL	P	P	P	P	P	P	P	S
19	Water	P	0.1 OG	P	IS	IS	IS	0.1 TL	IS	IS	P
20	DMSO/H ₂ O (75/25)**	S	S	2.0 OG	1.0	0.5 TL	0.5 TL	S	S	S	S
21	DMSO/H ₂ O (50/50)**	S	0.5 TL	0.1 TL	0.05	0.1 TL	0.25 TL	1.0 OG	P	P	S
22	DMSO/H ₂ O (25/75)**	S	0.1 TL	0.1 TL	0.25 TL	P	P	0.25 TL	IS	IS	S
23	EtOH/H ₂ O (75/25)**	S	S	S	S	2.0 OG	2.0 OG	S	S	S	S
24	EtOH/H ₂ O (50/50)**	S	1.0 OG	0.5 OG	0.5 OG	0.25 OG	0.25 TL	2.0	P	S	S
25	EtOH/H ₂ O (25/75)**	P	0.1 TL	0.1 TL	0.05 TL	P	P	0.25 OG	IS	IS	S

* TL, translucent gel; OG, opaque gel; S, solution; IS, insoluble; P, precipitation; PG, partial gel. ** Numbers in parentheses are the ratio of mixture solution (vol/vol). *** After 12 h.

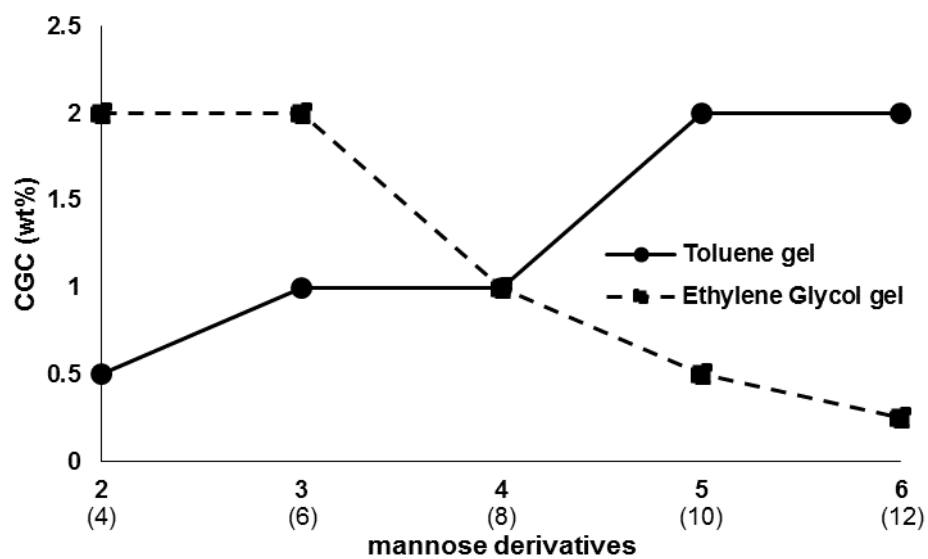


Figure 4. The CGCs of mannose derivatives, 2-6, in toluene and ethylene glycol (Numbers in parentheses are the length of alkoxy chain)

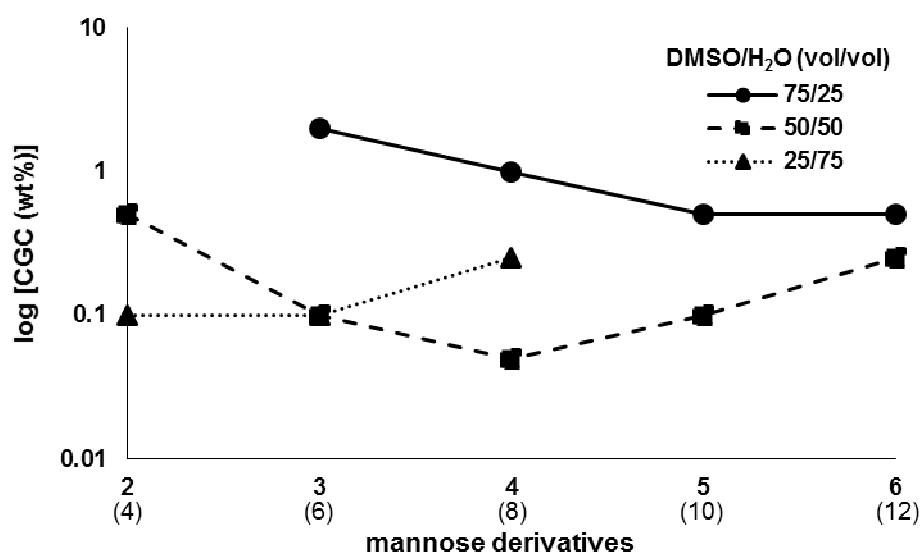


Figure 5. The CGCs of mannose derivatives, 2-6, in DMSO/H₂O mixtures (Numbers in parentheses are the length of alkoxy chain)

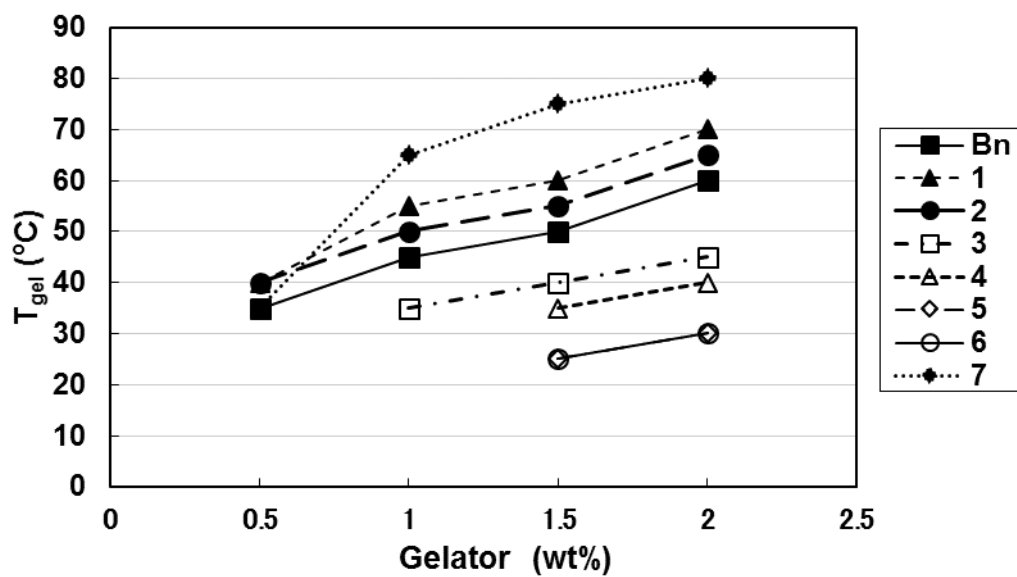
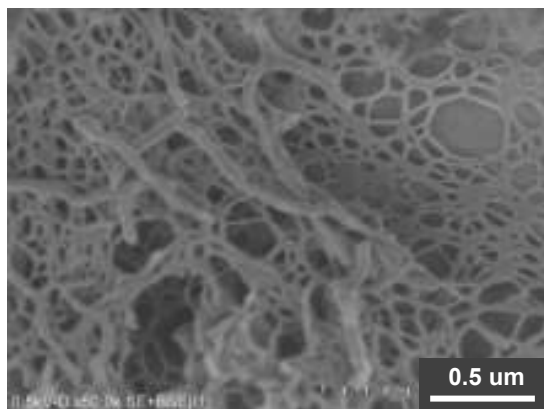


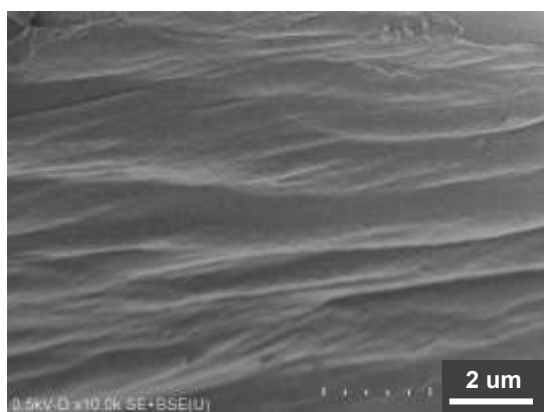
Figure 6. T_{gel} vs. gelator concentration in toluene



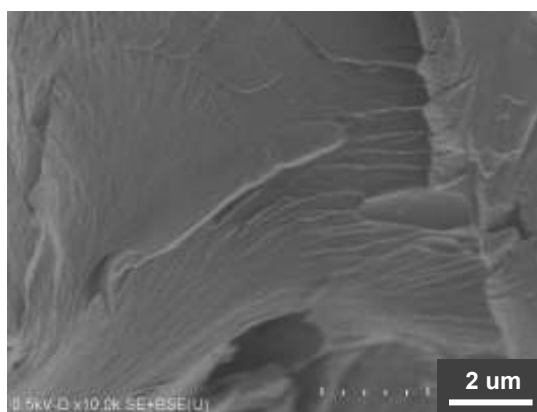
(a)



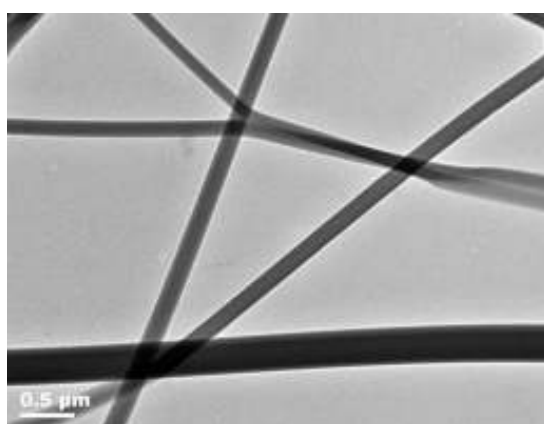
(b)



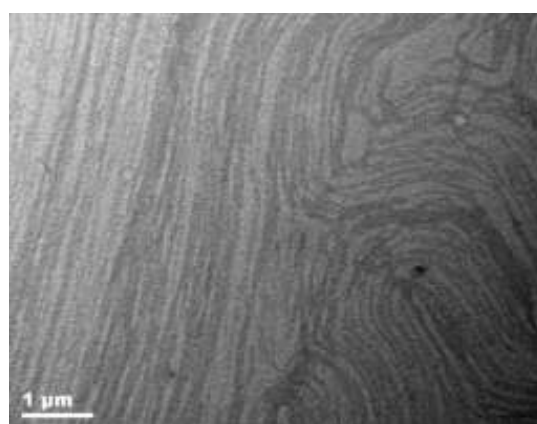
(c)



(d)



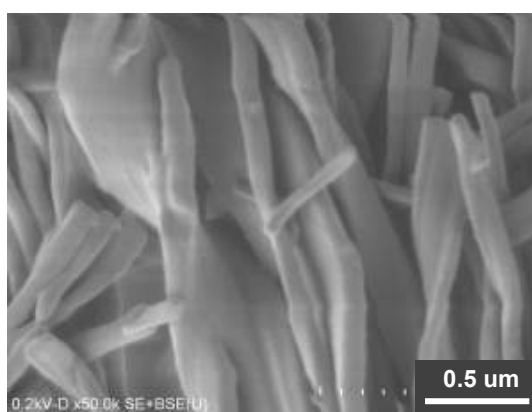
(e)



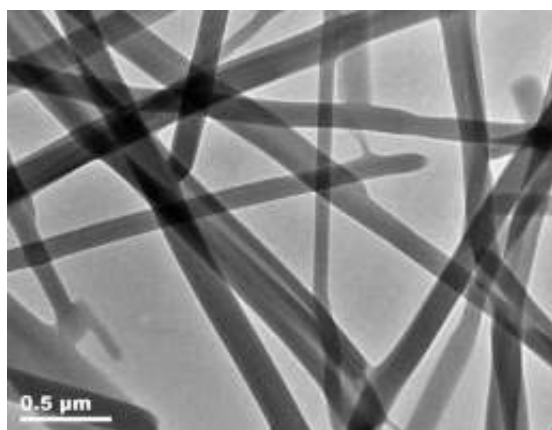
(f)



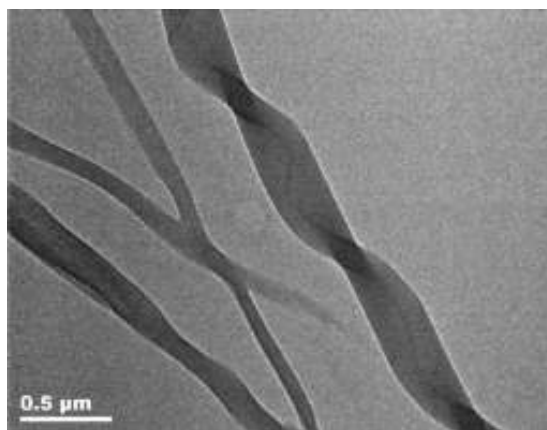
(g)



(h)



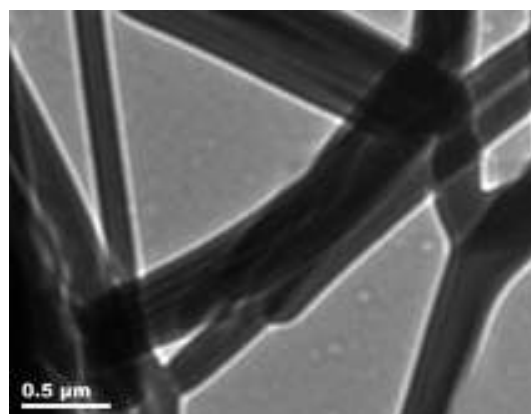
(i)



(j)



(k)



(l)

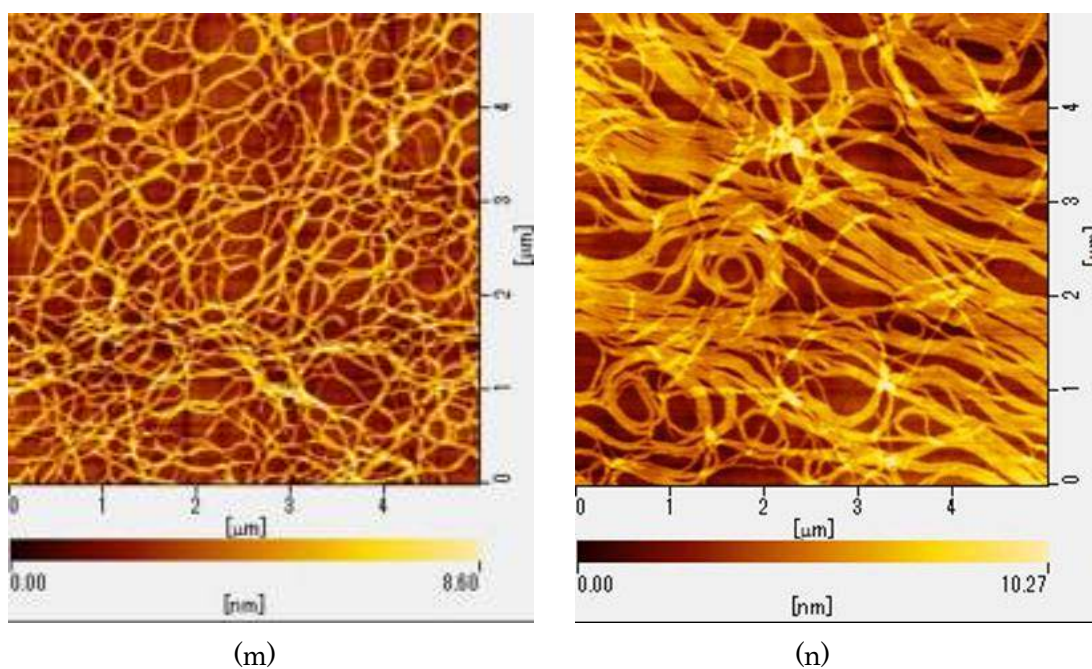


Figure 7. FE-SEM images of xerogels: cyclohexane with (a) **2** and (b) **6**; toluene with (c) **2** and (d) **6**; EtOH/H₂O (50/50, vol/vol) with (g) **2** and (h) **6**; and (k) hydrogel of **2**. TEM images gels as follows: toluene with (e) **2** and (f) **6**; EtOH/H₂O (50/50, vol/vol) with (i) **2** and (j) **6**; and (l) hydrogel of **2**. The AFM images of dried toluene solution of (m) **2** and (n) **6** at 0.02 wt% on HOPG

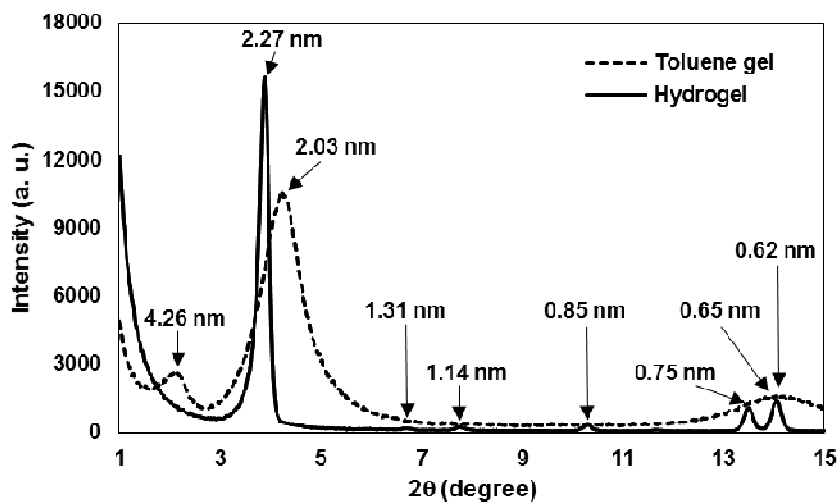


Figure 8. XRD measurements of the xerogels of organogel (toluene) and hydrogel prepared from **2**

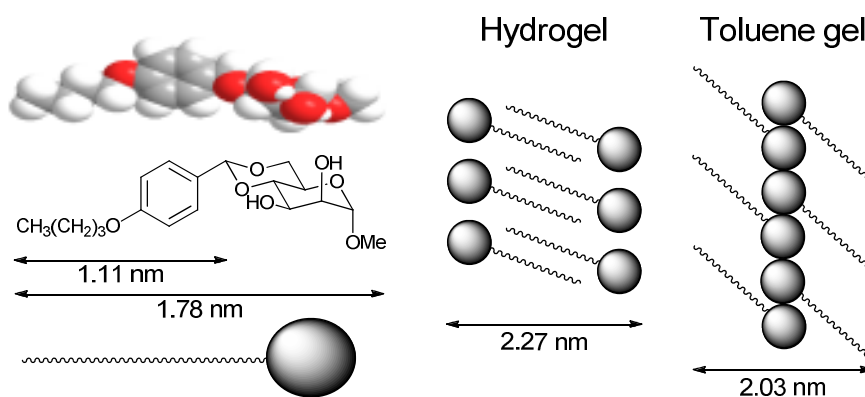


Figure 9. The molecular length of **4** by CPK molecular modelling on the basis of PM3 calculation and proposed molecular packing of **4** in hydrogel and toluene gel

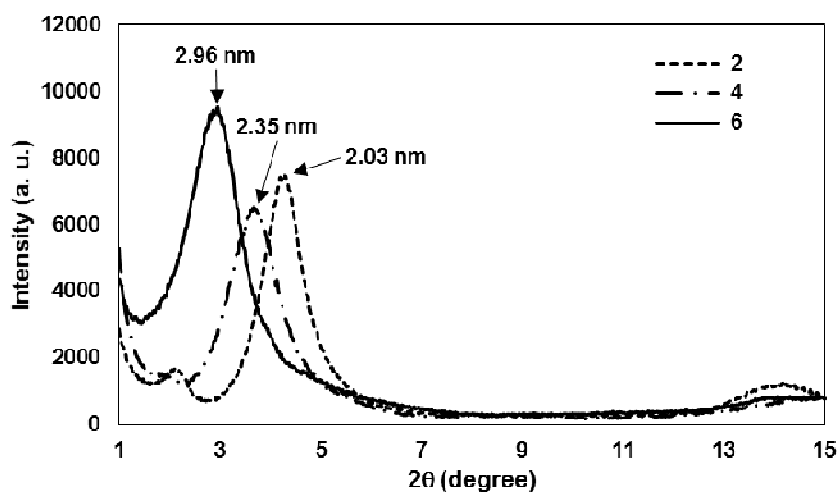


Figure 10. XRD measurements of the xerogels prepared from toluene with **2**, **4** and **6**



Figure 11. Thixotropic behaviour of organogels prepared from **3** with toluene (left), after shear stress (middle) and after 1 h at RT (right)

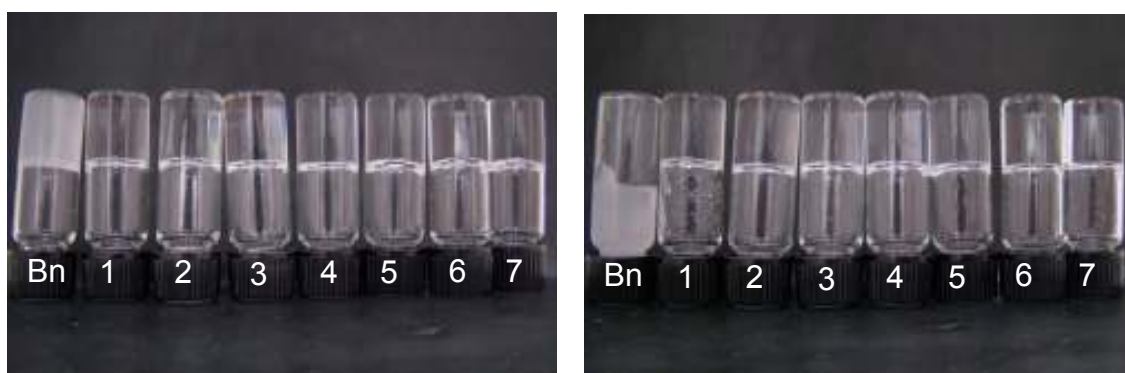


Figure 12. Thixotropic behaviours of organogels prepared from **Bn** and **1-7** with toluene (left) and after applying shear stress, then rest for 1 h at RT (right)

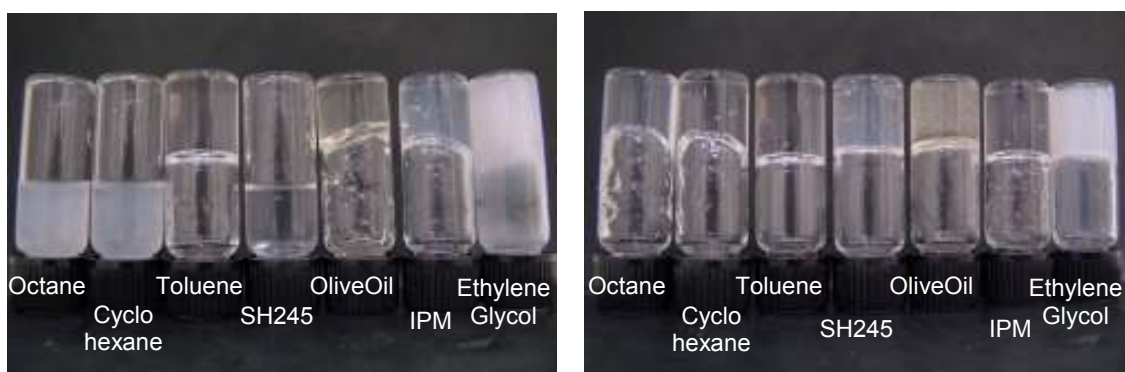


Figure 13. Thixotropic behaviours of several gels formed with several solvents and **2** (left) or **6** (right)

Structural optimization of super-gelators derived from naturally-occurring mannose and their morphological diversity

Fumiyasu Ono,^{*a} Hisayuki Watanabe^{a,b} and Seiji Shinkai^c

The mannose derivatives with various alkoxy substituents are able to gelate organic solvents and protic solvents. These gelators impart transparency, stability and thixotropic behavior for the gels.

